Electronic Supplementary Information for

Encapsulation of SnO_2 Nanocrystals into Hierarchically Porous Carbon by Melt Infiltration for High-Performance Lithium Storage

Li Shen,[a] Fang Liu,[a] Gen Chen,[a] Huihui Zhou,[a] Zaiyuan Le,[a] Hao Bin Wu,*[a] Ge Wang,[b] and Yunfeng Lu*[a]

[a]Chemical and Biomolecular Engineering, University of California, Los Angeles, California 90095, United States. *Email: hbwu@ucla.edu; luucla@ucla.edu

[b]Beijing Key Laboratory of Function Materials for Molecule & Structure Construction, School of Materials Science and Engineering, University of Science and Technology Beijing, Beijing 100083, PR China

Experimental section

Synthesis of hierarchically porous carbon (HPC): Typically, 2 g of sucrose was dissolved in 28 ml of 0.1 M HCl aqueous solution. Then 13 ml of colloidal silica (Snowtex-UP, Nissan Chemical) was added to form a homogeneous precursor solution. The solution was then sent through the aerosol atomizer to produce aerosol droplets by a nitrogen flow. The temperature of the heating zone was set at 400 °C. The resulting particles were collected by filter and then processed to carbonization by the following heating procedure: heating at 500 °C for 5 h and then at 900 ^{o}C for 5h with a heating rate of 5 °C min^{-1}. The resulting black carbon/silica composite particles were then repeatedly etched by 5% HF to remove silica templates. The resulting HPC particles were then filtered, rinsed several times with deionized water, and dried in an oven at 80 °C.

Synthesis of SnO_2-C composite: 100 mg of $SnCl_2$ (Sigma) was firstly grinded using a mortar. 60 mg of HPC was then added and homogeneously grinded with the fine $SnCl_2$ particles for 30 minutes. The mixture was then transferred to a glass vial and vacuumized for 30 minutes. The vial was sealed under vacuum and treated at 280 °C for 3 h with a heating rate of 20 °C min^{-1}. Finally, after cooling down, the vial was opened and further heated at 230 °C for 5 h in air with a heating rate of 10 °C min^{-1}.

Synthesis of SnO_2: SnO_2 was obtained by rapid combustion of as-synthesized SnO_2-C composite using a heating rate of 10 °C min^{-1} to 700 ^{o}C, and then cooling down naturally.

Materials characterizations: Nitrogen adsorption/desorption isotherms at 77 K were measured using a Micromeritics ASAP 2020 analyzer. Thermogravimetric analysis was conducted in air by holding at 120 ^{o}C for 20 minutes and ramping afterwards by 10 °C min^{-1} to 700 °C. X-ray diffraction measurements were carried out on a Rigaku X-ray powder diffractometer by using Cu Kα radiation. Scanning electron microscopy (SEM) images were obtained with a JEOL JSM-6700

FESEM. Transmission electron microscopy (TEM) images were obtained with a FEI T12 operated at 120 kV. High-resolution (HR) TEM and energy dispersive X-ray spectroscopy (EDX) analyses were performed on a FEI Titan S/TEM (300 kV for TEM imaging and 200 kV for STEM and EDX).

Electrochemical characterizations: The working electrodes were prepared by mixing SnO_2-C composite, super P, and sodium alginate with a mass ratio of 6:2:2 into a homogenously slurry with deionized water. The slurry was then pasted on a copper foil (MTI) using a doctor blade with a resulting mass loading of ~0.7-1 mg cm^{-2} (specific capacity is based on the mass of SnO_2-C composite). Electrodes for SnO_2 were prepared in the same way. The electrolyte was commercial 1M $LiPF_6$ in ethylene carbonate/diethyl carbonate (EC: DEC) with a volume ratio of 1:1. The half-cells were assembled using 2032-tpye coin cells in an argon-filled glove box by using lithium foil as counter electrode and glass fiber (GF/C, Whatman) as separator. The cyclic voltammetry curves were measured by Bio-logic VWP3 in a voltage window of 0.02-3 V at a scan rate of 0.5 mV s^{-1}. The galvanostatic discharge/charge tests were performed on LAND2001 battery test system at room temperature, and the voltage window was from 0.02 to 3 V (*vs.* Li/Li^+). The electrochemical impedance spectroscopy (EIS) was carried out in the frequency range from 100 kHz to 10 mHz on a Salatron 1860/1287.

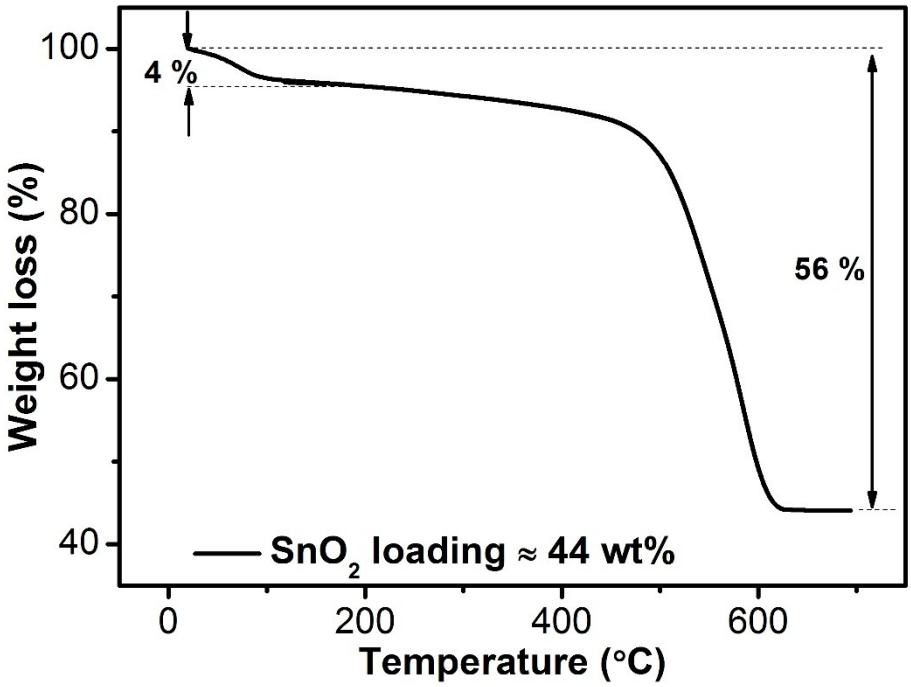

Fig. S1 TGA curve of SnO_2-C composite.

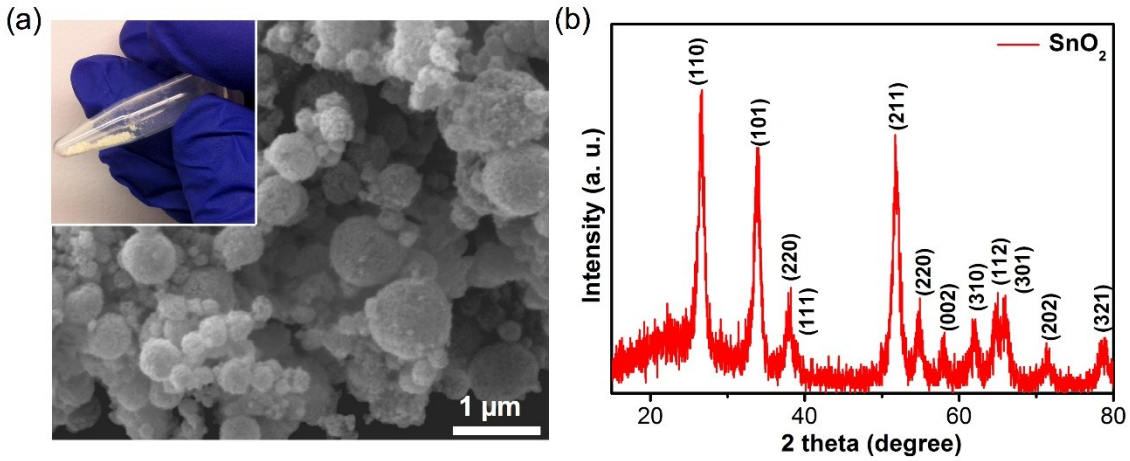

Fig. S2 (a) SEM image (inset: photograph) and (b) XRD pattern of SnO_2 obtained from combustion of SnO_2-C composite.

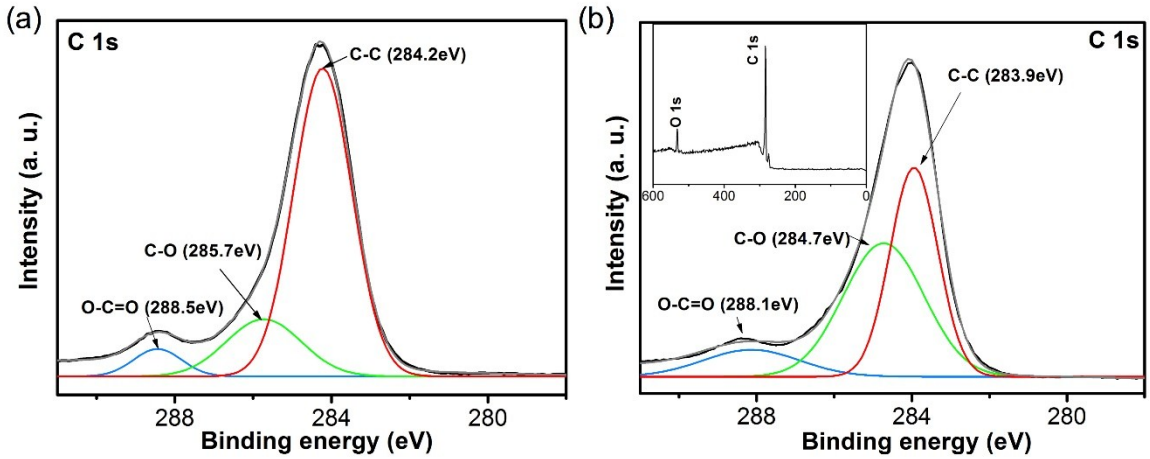

Fig. S3 C 1s spectra of (a) SnO_2-C composite and (b) HPC (inset: survey scan). The existence of oxygen is attributed to oxygen-containing functional groups on surface.

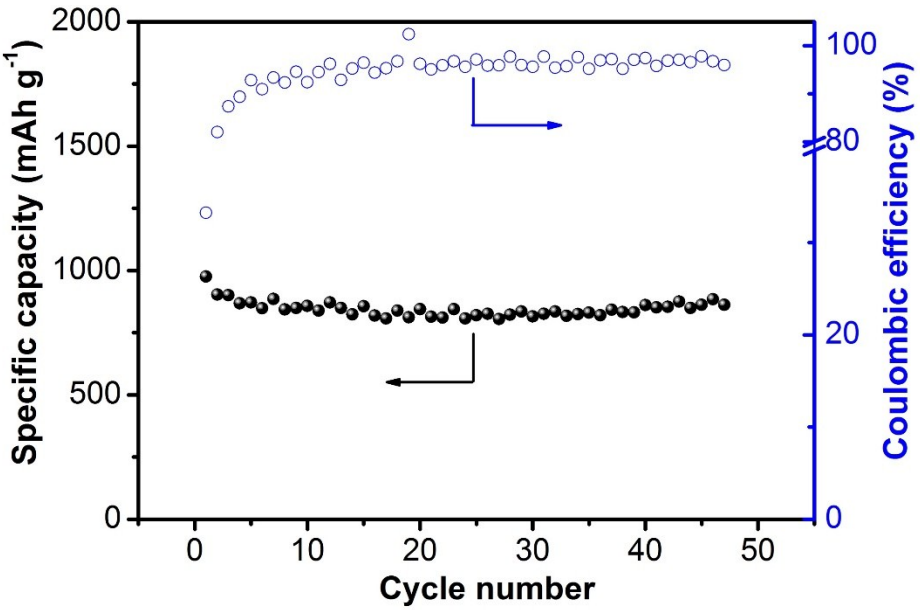

Fig. S4 Cycle performance of HPC at 0.2 A g^{-1}. Based on the capacity in the 10th cycle, the specific capacity of SnO_2 could be estimated using the following equation:
$C_{SnO_2} = (C_{SnO_2\text{-}C} - w\%_{HPC} * C_{HPC})/w\%_{SnO_2} = (964 - 0.56 * 843)/0.44 \approx 1120$ mAh g^{-1}
Although HPC can deliver rather high specific capacity by itself, the low Coulombic efficiency of ca. 95 % and low density make it unsuitable for practical use.

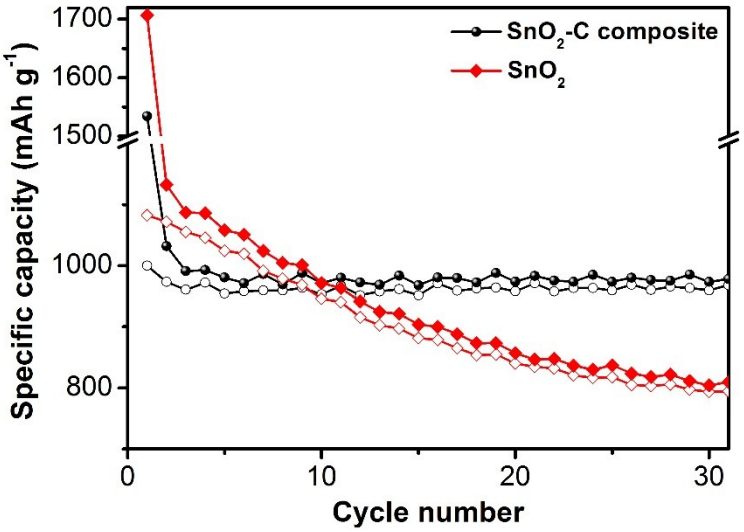

Fig. S5 Cycle performance comparison between SnO_2 and SnO_2-C composite (Voltage window: 0.02-3 V *vs.* Li/Li^+, current density: 0.2 A g^{-1}).

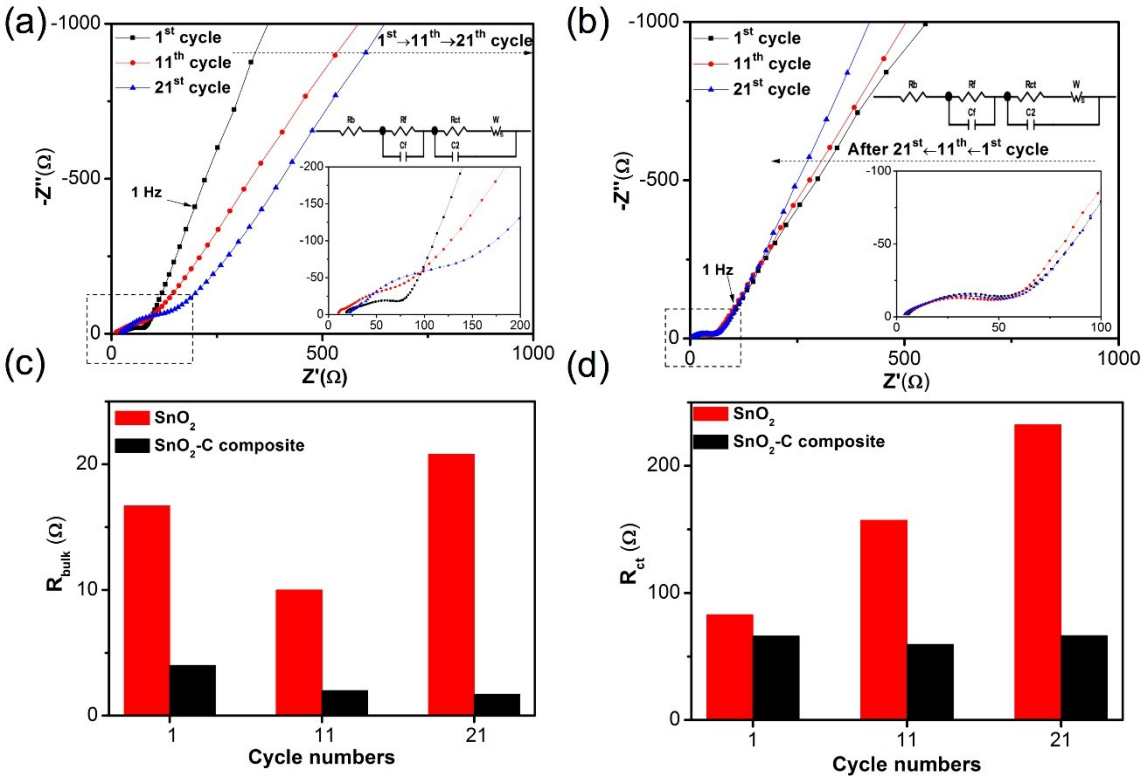

Fig. S6 EIS spectrums of (a) SnO_2 and (b) SnO_2-C composite after 1st, 11th and 21st cycle at 0.2 A g^{-1} (charged to 3V *vs.* Li/Li^+). Insets show magnified plots and equalivalent cicuirt model. Comparison of (c) Bulk resistance and (d) charge transfer resistance between SnO_2 and SnO_2-C composite**.**

Table S1. Comparison of surface area, pore volume and average pore size of HPC and SnO_2-C composite.

	BET surface area ($m^2\ g^{-1}$)	BJH pore volume ($cm^3\ g^{-1}$)	BJH average pore size (nm)
HPC	1349	3.84	10.7
SnO_2-C composite	689	1.32	6.7

Table S2. Electrochemical performance comparison of various SnO_2-based anodes.

SnO_2-based anodes	**Preparation methods**	**Cycling performances**	**Ref**
SnO_2@HPC	Melt infiltration of $SnCl_2$	1400 mAh g^{-1} (600th cycle) at 0.2 A g^{-1}	This work
Bowl-like SnO_2@Carbon	Hydrothermal	963 mAh g^{-1} (100th cycle) at 0.4 A g^{-1}	1
Tubular SnO_2@Carbon	Hydrothermal	700 mAh g^{-1} (50th cycle) at 0.2 A g^{-1} (0.05-1.5V)	2
SnO_2 nanotubes	Hydrothermal	513 mAh g^{-1} (50th cycle) at 0.4 A g^{-1} (0.005-1.2V)	3
Fluorine-doped SnO_2	Laser process	778 mAh g^{-1} (100th cycle) at 0.1 A g^{-1}	4
Antimony-doped SnO_2	Electrospinning	800 mAh g^{-1} (100th cycle) at 0.1 A g^{-1}	5
SnO_2@graphene	Hydrothermal	720 mAh g^{-1} (70th cycle) at 0.1 A g^{-1}	6
SnO_2@Mesoporous carbon	Wet impregnation of $SnCl_4{\cdot}5H_2O$	978 mAh g^{-1} (100th cycle) at 0.2 A g^{-1}	7
SnO_2@Tubular mesoporous carbon	Wet impregnation of $SnCl_4{\cdot}5H_2O$	630 mAh g^{-1} (50th cycle) at 0.5 A g^{-1}	8
SnO_2@Carbon nanotube	Wet impregnation of $SnCl_4{\cdot}5H_2O$	757 mAh g^{-1} (50th cycle) at 0.1 A g^{-1}	9
SnO_2 hollow nanospheres	Molten infiltration of $SnCl_2{\cdot}2H_2O$	700 mAh g^{-1} (20th cycle) at 0.16 A g^{-1}	10
SnO_2@Carbon nanotube	Wet impregnation of $SnCl_2{\cdot}2H_2O$	556 mAh g^{-1} (50th cycle) at 0.05 A g^{-1}	11
SnO_2@Carbon nanotube	Wet impregnation of $SnCl_2{\cdot}2H_2O$ under vacuum	430 mAh g^{-1} (300th cycle) at 0.1 A g^{-1}	12
SnO_2@Mesoporous carbon	Wet impregnation of $SnCl_2$	1145 mAh g^{-1} (30th cycle) at 0.08 A g^{-1}	13

Table S3. Cycle performance comparison between SnO_2 and SnO_2-C composite at 0.2 A g^{-1} for the first 20 cycles.

	Initial CE	Average CE[a]	Capacity retention
SnO_2	63.4%	97%	78%
SnO_2-C	65.2%	98%	100 %

[a] excluding the first cycle

References

1. J. Liang, X.-Y. Yu, H. Zhou, H. B. Wu, S. Ding and X. W. Lou, *Angew. Chem. Int. Ed.*, 2014, **53**, 12803-12807.
2. L. Zhang, G. Zhang, H. B. Wu, L. Yu and X. W. Lou, *Adv. Mater.*, 2013, **25**, 2589-2593.
3. X. Xu, J. Liang, H. Zhou, D. Lv, F. Liang, Z. Yang, S. Ding and D. Yu, *J. Mater. Chem. A*, 2013, **1**, 2995-2998.
4. J. H. Park, R. Kohler, W. Pfleging, W. Choi, H. J. Seifert and J. K. Lee, *RSC Adv.*, 2014, **4**, 4247-4252.
5. Y. S. Kim, W. B. Kim and Y. L. Joo, *J. Mater. Chem. A*, 2014, **2**, 8323-8327.
6. Z. Li, G. Wu, D. Liu, W. Wu, B. Jiang, J. Zheng, Y. Li, J. Li and M. Wu, *J. Mater. Chem. A*, 2014, **2**, 7471-7477.
7. F. Han, W.-C. Li, M.-R. Li and A.-H. Lu, *J. Mater. Chem.*, 2012, **22**, 9645-9651.
8. W.-H. Qu, F. Han, A.-H. Lu, C. Xing, M. Qiao and W.-C. Li, *J. Mater. Chem. A*, 2014, **2**, 6549-6557.
9. J. Xie, J. Yang and X. Zhou, *RSC Adv.*, 2014, **4**, 572-577.
10. S. Ding, J. S. Chen, G. Qi, X. Duan, Z. Wang, E. P. Giannelis, L. A. Archer and X. W. Lou, *J. Am. Chem. Soc.*, 2011, **133**, 21-23.
11. X. Liu, M. Wu, M. Li, X. Pan, J. Chen and X. Bao, *J. Mater. Chem. A*, 2013, **1**, 9527-9535.
12. R. Hu, W. Sun, H. Liu, M. Zeng and M. Zhu, *Nanoscale*, 2013, **5**, 11971-11979.
13. J. Chen and K. Yano, *ACS Appl. Mater. & Interfaces*, 2013, **5**, 7682-7687.